Cell, Vol. 101, 703–715, June 23, 2000, Copyright ©2000 by Cell Press

Repulsive Axon Guidance: Abelson and Enabled Play Opposing Roles Downstream of the Roundabout Receptor

Greg J. Bashaw,* Thomas Kidd,*§ Dave Murray,† Tony Pawson,† and Corey S. Goodman*‡

*Howard Hughes Medical Institute
Department of Molecular and Cell Biology
University of California, Berkeley
Berkeley, California 94720

†Samuel Lunenfeld Research Institute
Mt. Sinai Hospital
Toronto, Ontario M5G 1X5
Canada

Summary

***Drosophila* Roundabout (Robo) is the founding member of a conserved family of repulsive axon guidance receptors that respond to secreted Slit proteins. Little is known about the signaling mechanisms which function downstream of Robo to mediate repulsion. Here, we present genetic and biochemical evidence that the Abelson (Abl) tyrosine kinase and its substrate Enabled (Ena) play direct and opposing roles in Robo signal transduction. Genetic interactions support a model in which *Abl* functions to antagonize Robo signaling, while Ena is required in part for Robo's repulsive output. Both Abl and Ena can directly bind to Robo's cytoplasmic domain. A mutant form of Robo that interferes with Ena binding is partially impaired in Robo function, while a mutation in a conserved cytoplasmic tyrosine that can be phosphorylated by Abl generates a hyperactive Robo receptor.**

Introduction

Neuronal growth cones follow specific pathways and navigate a series of choice points to find their correct targets. At each decision point, growth cones encounter a plethora of guidance cues in their extracellular environment. Guidance decisions are shaped by a balance of both attractive and repulsive signals and these signals can act at short or long range (Tessier-Lavigne and Goodman, 1996). Many ligands and receptors have been discovered and have been found to be members of phylogenetically conserved protein families. An emergent theme from several recent studies is that often, ligands are indeterminate, capable of generating either attractive or repulsive responses, and that it is the type of receptor or receptor complex expressed on the surface of the growth cone that determines the response (Bashaw and Goodman, 1999; Hong et al., 1999). Cytoplasmic domain swaps between attractive Netrin and repulsive Slit receptors indicate that the sign of the growth cone response is encoded in the cytoplasmic domains of these receptors.

‡To whom correspondence should be addressed.
§Present address: Exelixis Pharmaceuticals, Inc., 260 Littlefield Avenue, South San Francisco, CA 94080.

If attraction versus repulsion is encoded in the cytoplasmic domain of the guidance receptor, then what are the signaling components within the growth cone that interact with a given receptor's cytoplasmic domain to generate specific outputs? To address this question, we have undertaken a genetic and biochemical analysis of the Roundabout (Robo) repulsive axon guidance receptor in *Drosophila* (Kidd et al., 1998a, 1998b).

Drosophila Robo is the founding member of a conserved family of repulsive axon guidance receptors (Kidd et al., 1998a; Zallen et al., 1998) that respond to secreted Slit proteins (Brose et al., 1999; Kidd et al., 1999; Li et al., 1999). Robo is a member of the immunoglobulin (Ig) superfamily and has an ectodomain with five Ig domains and three fibronectin (FN) type III repeats, a single transmembrane domain, and a long 457 amino acid cytoplasmic tail. The cytoplasmic domain does not contain any obvious catalytic signaling motif, but it does have proline-rich regions, potential phosphorylation sites, and other short stretches of evolutionarily conserved sequences (Kidd et al., 1998a). *robo* was identified in a mutant screen for genes that control the decision by axons to cross or not to cross the CNS midline (Seeger et al., 1993). In *robo* mutant embryos, too many axons cross and recross the midline.

How does Robo transmit its repulsive signal in response to Slit? A comparison of the *Drosophila* and Human Robo sequences revealed four short blocks of conserved cytoplasmic sequence, which were called CC0, CC1, CC2, and CC3 (CC for conserved cytoplasmic). CC2 (LPPPP) is a consensus binding site for the Ena-VASP-homology (EVH1) domain of *Drosophila* Enabled (Ena). Ena was originally identified in a screen for suppressors of mutations in the *abelson(abl)* tyrosine kinase (Gertler et al., 1995). Ena is a member of a small family of evolutionary conserved proteins that consist of an N-terminal EVH1 domain, a central proline-rich region which acts as a ligand for the actin monomer binding protein Profilin as well as several SH3 domain containing proteins including Abl (Reinhard et al., 1995; Gertler et al., 1996), and a C-terminal EVH2 domain involved in oligomerization and F-actin binding (Bachmann et al., 1999). It is expressed in CNS axons during *Drosophila* embryogenesis (Gertler et al., 1995).

Ena family members have been implicated in the regulation of the actin cytoskeleton during cell motility and growth cone guidance. For example, mammalian Ena (Mena) shows a striking localization to the distal tips of filopodia in cultured hippocampal neurons, and *mena* mutant mice have defects in the corpus collosum and the hippocampal commissure (Lanier et al., 1999). In the fly, mutations in *ena* lead to mild defects in CNS axon guidance and also result in defects in motor axon pathways (Wills et al., 1999b). Furthermore, the motility of the intracellular pathogen *Listeria monocytogenes* resulting from rapid actin polymerization at one pole of the bacterium requires Ena/VASP proteins (Laurent et al., 1999; Loisel et al., 1999).

These data from *Listeria*, coupled with observations

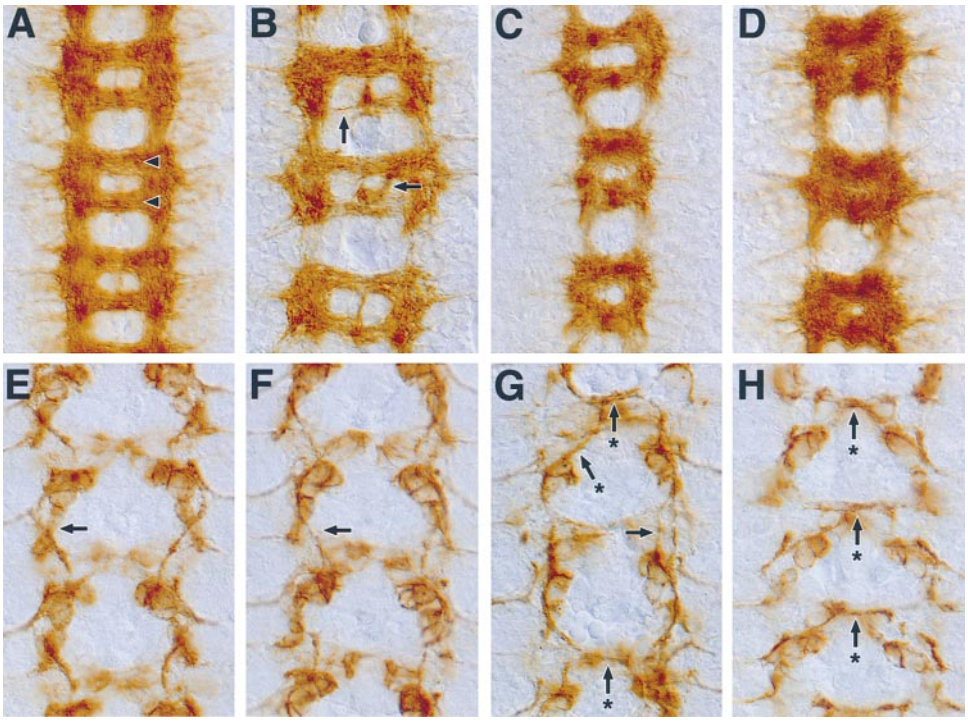

Figure 1. Dominant Enhancement of *ena* Loss-of-Function

Each panel shows three segments of the embryonic CNS. Anterior is up. The stage 16 embryos in (A)–(D) are stained with monoclonal antibody (Mab) BP102 to reveal the CNS axon scaffold. The stage 13 embryos in (E)–(G) are stained with anti-Fas II Mab to reveal the longitudinal pCC axon pathway. (A and E) Wild type. (B and F) ena^{210}/ena^{GC1}. (C and G) ena^{210}/ena^{GC1}, $robo^{4}/+$. (D and H) *robo4*.

(A) Arrowheads show the anterior and posterior commissures.

(B) Note the general disorganization of the CNS axon bundles. Arrows indicate typical deviations in commissural axon bundles.

(C) The bottom two segments have thicker than normal commissures and the longitudinal pathways show a marked lateral constriction towards the midline.

(D) Commissures are much thicker and appear fused. Longitudinal pathways are reduced and constricted laterally.

(E) The arrow indicates the pCC axon, which extends anteriorly and slightly away from the midline.

(F) pCC behaves normally.

(G) The pCC axon inappropriately crosses the midline in the top and bottom segments (arrows with asterisks). In the middle segment, pCC has a normal trajectory (arrow).

(H) The pCC axon inappropriately crosses the midline in every segment (arrows with asterisks).

that Ena family members can nucleate actin polymerization and bundle actin in vitro, have led to the suggestion that Ena/VASP proteins stimulate actin polymerization and cell motility. However, the presence of an Ena binding site in a repulsive guidance receptor points to a more complex role for Ena/VASP function. Does Ena lead to an increase or decrease in motility? Is Ena involved in attraction or repulsion? The results we present here strongly implicate Ena in repulsive axon guidance downstream of Robo. In a companion paper, Bear and colleagues (Bear et al., 2000 [this issue of *Cell*]) show that inhibition of Ena/VASP function actually increases the rate of cell migration of cultured fibroblasts, and that increased levels of Mena slow cells down. These two papers challenge the notion that Ena/VASP proteins play a stimulatory role in whole cell and growth cone motility, and instead focus attention on their role in repulsion and inhibition.

In the fly, mutations in the two genes—*ena* and *robo*—display strikingly different phenotypes; *ena* is weaker than *robo* in terms of midline guidance defects, but *ena* affects a broader range of guidance decisions than *robo*. Thus, if Ena functions downstream of Robo, then it can not function in a one receptor/one adaptor linear pathway. To determine if Ena plays a more subtle role in Robo signaling, we looked for genetic and biochemical interactions between Robo and Ena. *ena* and *robo* show several dosage-sensitive genetic interactions. In light of the known interactions between Ena and the Abl tyrosine kinase, the observation that *robo* interacts with *ena* suggested that Abl too could be involved in Robo signaling. While we were testing for *robo/ena* interactions, we recovered *abl* in a screen for genes that could modify the Fra-Robo chimeric receptor overexpression phenotype. This convergence led us to examine interactions between Robo and Abl as well.

A role for Abl in CNS axon guidance has been previously revealed by removing *abl* and a number of other gene functions (Gertler et al., 1989). For example, double mutants of *abl* and *Fasciclin I* show a dramatic reduction in the thickness of commissural axon bundles (Elkins et al., 1990). Like *ena*, mutations in *abl* also alter ISNb motor axon guidance (Wills et al., 1999a). Here, we show that whereas Ena mediates part of Robo's repulsive signal, in contrast, Abl antagonizes Robo signaling.

Both Abl and Ena can directly bind to Robo's cyto-

Table 1A. Dominant Enhancement of *ena*

Genotype	Segments scored	Thicker commissures	Segments with lateral constriction
ena^{210}/ena^{GC1}	77	8%	1.3%
$ena^{210}/ena^{GC1};robo^{4}/+$	209	37%	25%

Stage 15–16 embryos stained with MAb BP102 were scored.

plasmic domain. A mutant form of Robo which interferes with Ena binding has impaired function, while a mutation in a conserved cytoplasmic tyrosine that can be phosphorylated by Abl generates a hyperactive Robo receptor. Taken together, our genetic and biochemical data are consistent with a model in which Abl and Ena play direct and opposing roles in Robo mediated repulsion.

Results

Reducing *robo* Gene Dose in *ena* Mutants Reveals a Role for *ena* in Midline Repulsion

In wild-type embryos, the CNS axon scaffold has a characteristic ladder-like appearance with longitudinal axon bundles running along either side of the midline and commissural axon bundles crossing the midline in the anterior and posterior commissures in each segment (Figure 1A). In *ena* mutants, the overall pattern of the CNS axon scaffold is fairly normal; the longitudinal axon tracks and anterior and posterior commissures are spaced normally and are usually of wild-type thickness. However, in contrast to wild type, the axons in *ena* mutants appear to be less tightly fasciculated, and commissural bundles sometimes appear abnormal and wander between commissures (Figure 1B) (Gertler et al., 1995). Also, there are occasional errors in midline guidance, and axon pathways that do not normally cross the midline sometimes do (Table 1). Mutations in *robo* dramatically disrupt the CNS axon scaffold, causing far too many axons to cross and recross the midline; anterior and posterior commissures appear to be much thicker, or even fused together, and the longitudinal connectives are greatly reduced (Figure 1D) (Seeger et al., 1993).

To see if *ena* could play a role in Robo-mediated repulsion that is not apparent in animals mutant for *ena* alone, we reduced *robo* gene dose in *ena* mutants. We find that *ena* mutants that are heterozygous for mutations in *robo* exhibit striking defects in CNS axon guidance, indicative of a loss of midline repulsion; the anterior and posterior commissures are significantly thicker, longitudinal connectives are reduced and are sometimes closer to the midline. These animals have variable phenotypes, with some segments showing defects that approach those seen in animals that completely lack *robo* function (Figure 1C and Table 1A). We also looked at the axons that pioneer one of the longitudinal axon pathways. Normally, the pCC cell body, positioned at a distance of several cell diameters from the midline, extends an axon anteriorly to join with descending axons from the MP1 and dMP2 neurons. Together these axons pioneer the pCC pathway, which runs parallel to but does not cross the midline (Figure 1E). In *robo* mutants, pCC initially extends anteriorly, but instead of continuing its anterior trajectory, it turns and crosses the midline (Figure 1H). In *ena* mutants, pCC behaves normally. But if *ena* is mutant, and *robo* is reduced by 50%, then

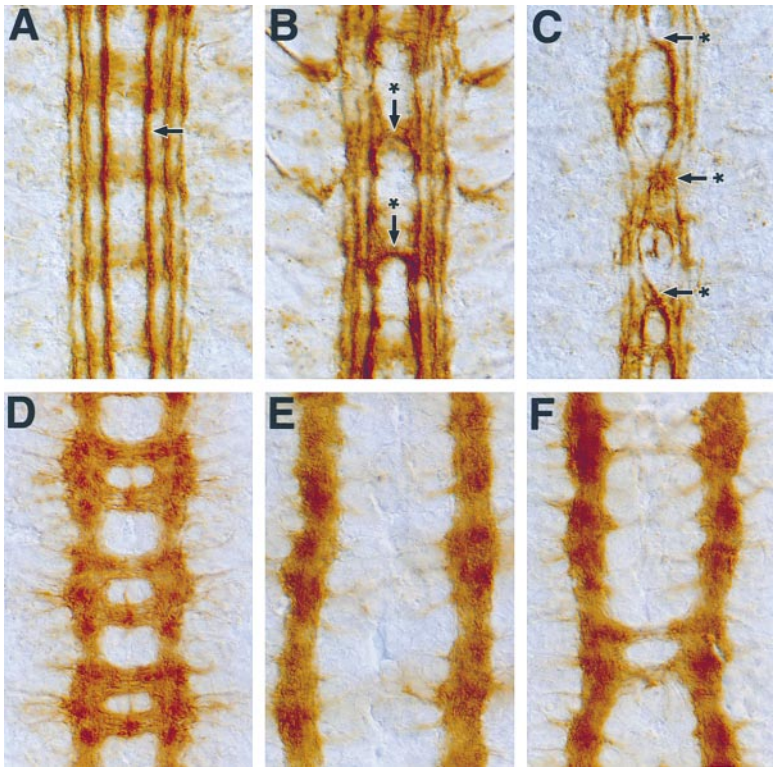

Figure 2. Genetic Interactions between *ena*, *slit*, and *robo*

(A–C) Late stage 16 embryos stained with anti-Fas II Mab to reveal longitudinal axon pathways. Anterior is up. (A) A wild-type embryo. The arrow indicates the medial longitudinal pathway. No Fas II-positive axon bundles cross the midline. (B) A $slit^{1},robo^{5}/++$ transheterozygous embryo with mild midline crossing defects. Arrows with asterisks indicate axon bundles that are inappropriately crossing the midline. (C) A $slit^{1},robo^{5},+/+.+,ena^{GC1}$ embryo with severe midline crossing defects. The medial axon pathway wanders back and forth across the midline (arrows with asterisks).

(D–F) Stage 16 embryos stained with Mab BP102. (D) A wild-type embryo. (E) A *UAS-roboY-F/elavGAL4* embryo. Commissural axon pathways are absent. (F) The same genotype as in (E), but also heterozygous for the ena^{GC1} allele. Removing one copy of *ena* partially suppresses the commissureless phenotype.

Table 1B. Suppression of Gain-of-Function Phenotypes

Partial genotype	Segments scored	Commissures				
		Absent	Thin	Wild type	Thick	Deviant
UASroboY-F	110	95%	3.6%	1.4%	0%	0%
UASroboY-F;ena^{GC1}/+	132	76%	13%	7%	1%	3%
UASfra-robo	99	90%	10%	0%	0%	0%
UASfra-robo;ena^{GC1}	66	39%	29%	16%	0%	16%
EProbo2	144	29%	45%	16%	8%	8%
EProbo2,ena^{GC1}	84	11%	20%	25%	42%	2%
comm	121	99%	1%	0%	0%	0%
ena^{GC1};comm	88	76%	11%	4.5%	1%	7.5%

Stage 15–16 embryos stained with MAb BP102 were scored.

pCC frequently crosses the midline (Figures 1F and 1G). Normally, heterozygosity for *robo* does not cause defects. This kind of dose-sensitive genetic interaction, referred to as dominant enhancement, is often observed when two genes function together in the same process.

Complementary Dosage-Sensitive Genetic Interactions between *slit*, *robo*, and *ena*

Another common genetic test is to determine if 50% reduction of two genes reveals a phenotype not observed in the individual heterozygous mutants. This kind of transheterozygous interaction is very specific and is usually indicative of direct interaction in a common process. For example, *robo* and its ligand *slit* display such an interaction (Kidd et al., 1999).

We generated transheterozygous combinations of *robo* and *ena*, but we never observed significant ectopic midline crossing in these animals (Table 1C). Similar transheterozygous tests with *slit* and *ena* mutants revealed mild, but significant, midline crossing defects (Table 1C). Reasoning that a 50% reduction of either *robo* or *slit* alone did not create a sufficiently sensitized genetic background to see strong effects of reducing *ena* levels, we limited the gene dose of *slit, robo* and *ena*.

Transheterozygous *slit,robo/+* embryos typically display two to four axon bundles of the medial longitudinal pathway inappropriately crossing the midline per animal; such defects are never observed in wild-type embryos (Figures 2A and 2B; Table 1B). If now in this *slit,robo* background we also reduce *ena* by 50% a dramatic enhancement of the *slit,robo* phenotype is revealed; instead of 2–4 crossovers per embryo of the medial longitudinal pathway, we now see many more crossovers, often several per segment (Figure 2C and Table 1C). Thus, on the background of a 50% reduction in both ligand and receptor, we see a dramatic increase in inappropriate midline crossing by removing 50% of Ena. These observations further support a role for *ena* in *robo*-mediated repulsion.

We have also examined whether loss or reduction of *ena* function can suppress *robo* gain-of-function phenotypes. High level panneural expression of Robo generates a commissureless phenotype indicating that Robo repulsion can overcome all endogenous attraction to the midline (Figure 2E). This gain-of-function phenotype can be generated by overexpressing either wild-type Robo (Kidd et al., 1999), a mutated form of Robo, the Fra-Robo chimera (Bashaw and Goodman, 1999), or Robo2 (J. Simpson, personal communication). Furthermore, loss of *commissureless(comm)* function arguably represents the ultimate gain of *robo* function, since in the absence of Comm, Robo can not be down-regulated on commissural axons (Kidd et al., 1998b).

ena can partially suppress all of these types of gain-of-function *robo* phenotypes. With the exception of the tyrosine-phenylalanine (Y-F) mutant form of Robo (see transgenic expression of mutant forms of Robo below), significant suppression of the commissureless phenotype is not observed unless both copies of *ena* are removed (Table 1B). The suppression of the phenotype of the Y-F mutant receptor is most striking, where 50% reduction of *ena* function allows significant commissure formation (Figure 2F and Table 1B). These observations complement the dominant enhancement data, and together the genetic interaction results provide strong evidence that *robo* and *ena* work together in a common pathway to mediate midline repulsion.

Table 1C. Genetic Interactions between *ena, robo* and *slit***

Genotype	Segments scored	+	++	+++	Defects/animal	Defects (%)
ena^{210}/ena^{GC1}	143	18	15	3	2.8	23%
slit^{2}/ena^{210}	88	4	1	2	1	8%
robo^{4}, ena^{GC1}/+	66	0	0	0	0	0%
slit^{2}, +, +/robo^{4}, ena^{GC1}	143	44	50	41	10.4	67%
slit^{1},robo^{5}/+	231	32	27	8	3.2	29%
slit^{1},robo^{5},+/+,+, ena^{GC1}	121	31	62	44	12	74%
slit^{1},robo^{5},+/+,+, ena^{GC5}	110	27	35	18	8	69%
slit^{1},robo^{5},+/+,+, ena^{GC8}	187	43	55	47	8.5	70%

Stage 16–17 embryos stained with anti-FasII MAb were scored. Column designations are as follows: +, thinner than normal fascicle ectopically crossing the midline; ++, normal fascicle ectopically crossing the midline; +++, thicker than normal fascicle ectopically crossing the midline. **, neither *slit, robo,* nor *ena* show significant ectopic midline crossing as individual heterozygotes (data not shown).

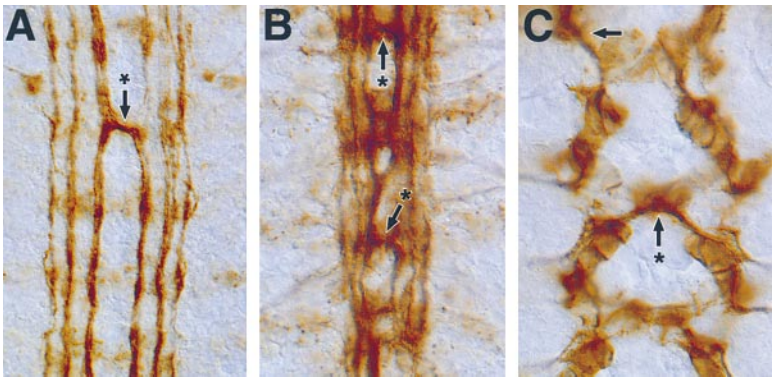

Figure 3. Abl Overexpression CNS Phenotypes

All preparations are stained with anti-Fas II MAb to reveal longitudinal axon pathways. Anterior is up.

(A) A late stage 16 embryo carrying one copy of *EPabl* and one copy of *elavGAL4*. One bundle of the medial pathway is ectopically crossing the midline (arrow with asterisk).

(B) A similar stage embryo as in (A) expressing higher levels of Abl. More severe midline crossing defects reminiscent of *robo* mutants are seen. Regions that show ectopic midline crossing are indicated by arrows with asterisks.

(C) A stage 13 embryo expressing high levels of Abl. The pCC axons on both sides of the central segment have inappropriately crossed the midline (arrow with asterisk). Compare with the normal trajectory of pCC in the top segment (arrow).

Overexpression of Abl Mimics *robo* Loss-of-Function

Overexpression of the Fra-Robo chimeric receptor leads to dose dependent CNS axon guidance defects and reduced viability. We screened the EP collection (a collection of P-element inserts that allows targeted misexpression of flanking genes) (Rørth, 1996) for genes that when overexpressed in combination with Fra-Robo, would enhance the lethality of the chimera. In this screen, we recovered an EP insert in *abl* as one strong enhancer. This finding was intriguing in light of the genetic interactions between *robo* and *ena*, and prompted us to investigate a role for Abl in Robo signaling.

We used the EP insert in *abl* to overexpress Abl in all neurons with *elavGAL4* and *scabrousGAL4*, and examined the CNS with antibodies to Fas II and BP102. Varying the copy number of EP*abl* and GAL4 driver allowed us to generate animals with a range of Abl expression levels. Overexpression of Abl results in dose-dependent ectopic midline crossing reminiscent of the phenotype observed in *robo* mutants. Low levels of Abl expression result in occasional errors in midline guidance; Fas II-positive bundles are sometimes observed to inappropriately cross the midline (Figure 3A and Table 1D). Higher levels of Abl expression caused more dramatic phenotypes that appear similar to loss of *robo* function (Figure 3B). Similar results were obtained with both GAL4 drivers, and substituting UAS*abl* for EP*abl* also gave comparable results (Table 1D and data not shown). Overexpression of Abl also disrupts the guidance of axons that pioneer the longitudinal pathways (e.g., the pCC neuron), causing them to inappropriately cross the midline (Figure 3C). The midline crossing defects caused by Abl overexpression are largely kinase dependent; only very weak effects are observed when a mutant form of Abl that lacks kinase activity (Henkemeyer et al., 1990) is similarly overexpressed (data not shown). This suggests that phosphorylation of substrates by Abl is important in generating the Abl overexpression phenotype.

Reducing Robo Function Enhances the Abl Overexpression Phenotype

The Abl overexpression phenotype suggests that Abl could act to antagonize Robo function. We reasoned that if increasing Abl expression produced its effects by directly antagonizing Robo, then genetically limiting *robo* and/or *slit* copy number might enhance the *abl* overexpression phenotype. We used low level expression of Abl (i.e., single copy), with the idea that it would be easy to detect enhancement of the mild phenotype caused by these levels of Abl. Indeed, although we

Table 1D. Genetic Interactions between *abl, robo* and *slit*

Genotype	Segments scored	+	++	+++	Defects/animal	Defects (%)
EPabl/elav	198	16	2	1	1	9%
UASabl/elav	176	3	2	0	0.3	3%
UASabl^{kindead}/elav	88	0	0	0	0	0%
ena^{GC1}/+EPabl/elav	154	7	2	1	0.7	6%
robo^{1}/+;EPabl/elav	99	30	38	13	9	74%
robo^{1}/+;UASabl/elav	176	40	32	9	5	43%
robo^{1}/+;UASabl^{kindead}	66	0	0	0	0	0%
slit^{2}/+;EPabl/elav	176	51	41	23	7.2	58%
slit^{1},robo^{5}/+;EPabl,elav	88	35	52	23	13.8	84%
UASroboΔC;EPabl,elav	110	26	22	6	5.4	45%
slit^{1},robo^{5}/+	231	32	27	8	3.2	29%
slit^{1},robo^{5}/+;abl^{1}/+	176	21	5	0	1.6	15%

Stage 16–17 embryos stained with anti-FasII MAb were scored. Column designations are as follows: +, thinner than normal fascicle ectopically crossing the midline; ++, normal fascicle ectopically crossing the midline; +++, thicker than normal fascicle ectopically crossing the midline.

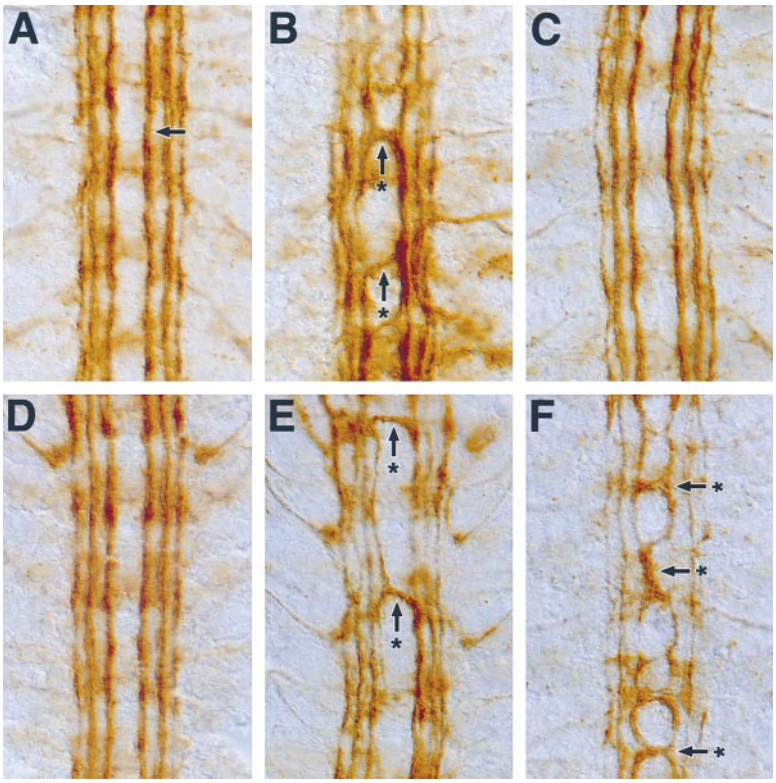

Figure 4. Genetic Interactions between *abl*, *slit*, and *robo*

Late stage 16 embryos stained with anti-Fas II MAb to reveal longitudinal axon pathways. Anterior is up.

(A) A *UASabl/elavGAL4* embryo. Note the wild-type appearance of the longitudinal pathways.

(B) A *robo/+; UASabl/elavGAL4* embryo. Removing a copy of *robo* enhances the midline defects caused by Abl overexpression (arrows with asterisks).

(C) A *robo/+; UASabl$^{kinase\ dead}$/elavGAL4* embryo. Overexpression of kinase dead Abl in a *robo* heterozygote does not result in significant defects.

(D) A *slit^{1},robo^{5}/++*; *abl^{1}/+* embryo. Removing a copy of *abl* partially suppresses the *slit,robo* transheterozygous phenotype. Note the wild-type appearance of the longitudinal pathways and compare with (E).

(E) A *slit^{1}*,robo^{5}/++ embryo. Arrows with asterisks indicate inappropriate midline crossovers.

(F) A *slit^{1}*,robo^{5}/++; *EPabl,elavGAL4* embryo. The midline crossing defects of *slit1, robo5/++* are enhanced by overexpression of Abl. (arrows with asterisks).

sometimes observe ectopic midline crossing in this background (Figure 3A and Table 1D), most animals carrying one copy of EP*abl* and one copy of *elavGAL4* are essentially wild type (Figure 4A and Table 1D). If, in this background we also remove one copy of *robo*, we see a marked enhancement of the midline crossing defects, with some animals showing many inappropriate cross-overs (Figure 4B and Table 1D). This effect is observed with two independent *robo* alleles (data not shown). Removing one copy of *slit* has a similar, but slightly weaker, effect. In addition, simultaneous panneural expression of Abl and a truncated Robo receptor, which acts as a weak dominant-negative, also enhances the ectopic midline crossing phenotype (Table 1D).

Interestingly, the phenotype resulting from increasing Abl and decreasing Robo is dependent on an intact Abl kinase domain; overexpressing a kinase-dead Abl in *robo* heterozygotes does not cause significant guidance errors (Figure 4C and Table 1D). This observation again suggests that phosphorylation of Abl substrates is important in generating these phenotypes. Removing one copy of *ena*, a known substrate of Abl and a logical candidate to be a potentially important target of Abl kinase activity in the context of midline repulsion, does not enhance the Abl overexpression phenotype (Table 1D), whereas removing one copy of *robo* does (Figure 4B and Table 1D).

Another prediction of the model that Abl inhibits Robo signaling is that decreasing Abl function could lead to an increase in Robo activity. To see if reducing *abl* gene dose could suppress the effects of partial loss of *robo* function, we tested whether removing one copy of *abl* could suppress the *slit,robo/+* transheterozygous phenotype. We found that reducing *abl* (using either the *abl1* or *abl4* allele) results in significant suppression of the *slit,robo/+* midline crossing defects (compare Figure 4D to 4E; Table 1D; and data not shown), arguing further for a role of *abl* in regulating Robo signaling. In contrast, increasing *abl* in the *slit,robo/+* background has the reciprocal effect of enhancing the midline crossing phenotype (Figure 4F and Table 1D).

Both Abl and Ena Can Bind to the Cytoplasmic Domain of Robo

To test whether the genetic interactions observed between *abl, ena*, and *robo* could reflect direct interaction between these three proteins, we have performed in vitro and in vivo assays for protein/protein interactions. For these experiments, a panel of Abl, Ena, and Robo protein expression constructs were generated (Figure 5A).

GST pull down assays reveal robust in vitro interactions between Ena and Robo, as well as Abl and Robo (Figures 5B–5D). In the case of Ena, bidirectional interactions have been examined: a GST Robo cytoplasmic domain fusion (GST RoboC) can effectively pull down in vitro translated Ena, while GST alone can not, and GST Ena can bind in vitro translated Robo, while GST alone can not (Figures 5B and 5C). In both cases, deletion of the CC2 motif results in a similar significant reduction in Robo/Ena binding, while mutations in either CC3 or the Y-F mutant in CC1 do not (Figures 5B and 5C). In addition, deletion of the CC1 motif also results in decreased binding of Ena, suggesting that there might be multiple sites of association between Ena and Robo. These interactions are observed in the context of full-length Ena, as well as with the isolated Ena EVH1 domain (Figure 5D).

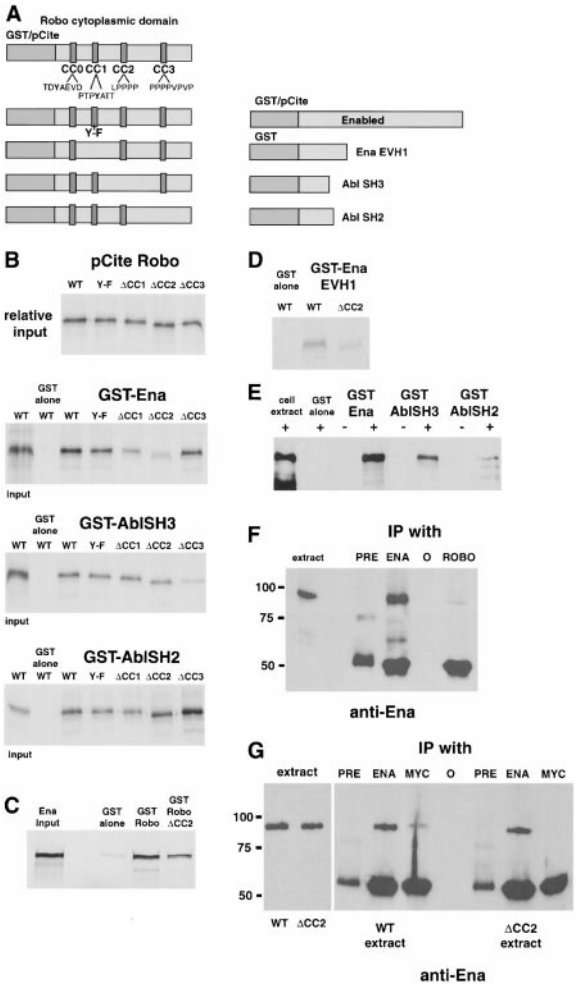

Figure 5. Ena and Abl Bind Robo's Cytoplasmic Domain

(A) A diagram of constructs used for in vitro binding assays. The left column shows Robo cytoplasmic domain constructs. The positions and sequences of the four CC motifs are indicated. Tyrosines (Y) in CC0 and CC1 that can be phosphorylated in vitro are in bold. The right column shows Abl and Ena constructs. GST/pCite indicates that two versions of the plasmids were made.

(B) Pull-down assays using GST Ena and Abl fusions and in vitro translated Robo cytoplasmic domains. The relative input of each version of Robo is shown in the top panel indicated above each lane. Breaks in panels are due to removal of irrelevant lanes. The fusion protein used is indicated above each gel. None of the pCite Robo products bind to GST alone. GST-Ena shows reduced binding to both ΔCC1 and ΔCC2—the reduction is more pronounced for ΔCC2. GST-AblSH3 shows reduced binding to ΔCC3.

(C) Pull down assays using GST-Robo and in vitro translated Ena. A small amount of Ena is bound by GST alone. GST-Robo binds much more strongly to Ena and this binding is reduced in the ΔCC2 mutant.

(D) Similar interactions are detected using the isolated Ena EVH1 domain.

(E) GST pull downs from S2 cells transfected with and without Robo. The + or − indicates Robo-expressing cells (+) or control cells (−). Western blots were probed with anti-Robo monoclonal antibody. GST-Ena, GST-Abl SH3, and GST-Abl SH2 all pull down full-length Robo from S2 cell extracts, while GST alone does not.

(F) Coimmunoprecipitation of Robo and Ena from wild-type embryos. Lanes are indicated above the gel and sizes are indicated next to the gel. An aliquot of extract is included as a positive control for the detection of Ena in the far left lane.

GST Abl SH3 and GST Abl SH2 can also efficiently pull down in vitro translated Robo (Figure 5B). Binding of Robo to the Abl SH3 domain is strongly reduced when the CC3 motif is deleted, while the other mutant forms do not significantly effect the observed binding (Figure 5B). In contrast to the interactions of Ena and the Abl SH3 domain with Robo, none of the Robo cytoplasmic domain mutants consistently effect the binding observed with the Abl SH2 domain (Figure 5B). In addition to efficiently binding to in vitro translated Robo, the GST Ena, GST Abl SH3, and GST Abl SH2 can precipitate full-length Robo from Robo-expressing S2 cells (Figure 5E).

We also examined in vivo interactions between Robo and Ena by coimmunoprecipitation from embryonic extracts. For this we generated a monoclonal antibody to the N terminus of Ena and used the previously described Robo monoclonal antibody. Our Ena antibody specifically recognizes Ena in whole-mount embryos as well as in extracts from embryos and S2 cells (Figures 5F and 5G; data not shown). Extracts were prepared from wild-type embryos as well as embryos expressing myc-tagged forms of Robo. We found that in wild-type embryonic extracts, the Robo monoclonal antibody can coimmunoprecipitate a small amount of Ena protein, while a preimmune serum can not (Figure 5F). In addition, in extracts from embryos expressing myc-tagged Robo, the anti-myc monoclonal antibody can also precipitate a small amount of Ena. Furthermore, in extracts from embryos expressing an equivalent amount of the myc-tagged RoboΔCC2 mutant, the myc antibody precipitates less Ena (Figure 5G). We have been unable to perform similar in vivo interaction experiments between Abl and Robo because we do not have an Abl antibody that efficiently recognizes Abl in embryonic extracts. However, the strong in vitro binding, together with the genetic interactions support the idea that Abl, like Ena, plays a direct role in Robo signal transduction.

Robo Is a Substrate for Abl Kinase Activity

To see if Abl could antagonize Robo by directly phosphorylating it, we tested whether Robo could be phosphorylated by Abl in mammalian Cos1 cell culture. When expressed in Cos1 cells, neither full-length human Robo1 (hRobo1), nor a Flag epitope-tagged hRobo1 cytoplasmic polypeptide, containing residues 930–1651 of the full-length protein, were detectably tyrosine phosphorylated. However cotransfection of a constitutively active c-Abl variant lacking the SH3 domain (Jackson and Baltimore, 1989), resulted in significant tyrosine phosphorylation of both full length hRobo1, as well as

(G) Coimmunoprecipitation of Ena with myc-tagged Robo proteins. Lanes are as indicated. The left half of the IP gel consists of immunoprecipitates from embryos expressing *UASrobomyc*, the right half of the IP gel is from embryos expressing *UASroboΔCC2myc*. Note the strong reduction of Ena signal in the Myc IP from the ΔCC2 extract. The two types of extracts contained similar amounts of Ena as shown in the small gel on the left.

(F and G) Ena protein is detected at the expected size of ~80 kDa. The strong signal at ~50 kDa in the IP lanes corresponds to mouse heavy chain.

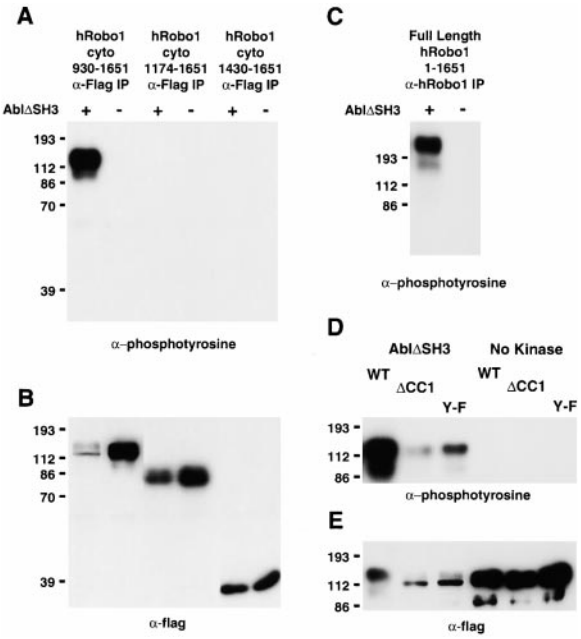

Figure 6. hRobo1 Is a Substrate for Abl in Cos1 Cells

(A and B) The hRobo1 cytoplasmic domain is tyrosine phosphorylated by active Abl in Cos1 cells. Flag-tagged cytoplasmic domain hRobo1 constructs were transfected alone, or in combination with AblΔSH3, into Cos1 cells as indicated. hRobo1 proteins were immunoprecipitated from cell lysates with an anti-Flag monoclonal antibody and analyzed by Western blotting using an anti-phosphotyrosine monoclonal antibody (A) or an anti-Flag monoclonal antibody (B). Lane designations in (B) are the same as those in (A). The breaks in the gels in (A) and (B) are due to removal of irrelevant lanes.

(C) Full-length hRobo1 is tyrosine phosphorylated by Abl. Full-length hRobo1 was transfected alone, or in combination with AblΔSH3 into Cos1 cells. hRobo1 was immunoprecipitated from cell lysates with an anti-hRobo1 polyclonal antibody and analyzed by Western blotting using an anti-phosphotyrosine monoclonal antibody.

(D and E) Decreased tyrosine phosphorylation of the hRobo1 cytoplasmic domain resulting from deletion of the CC1 motif or mutation of its conserved tyrosine. Wild-type, ΔCC1, or Y1073F hRobo1 cytoplasmic domain constructs were transfected alone or in combination with AblΔSH3 into Cos1 cells. hRobo1 proteins were immunoprecipitated from cell lysates with an anti-Flag monoclonal antibody and analyzed by Western blotting using an anti-phosphotyrosine monoclonal antibody (D) or an anti-Flag monoclonal antibody (E). Lane designations in (E) are the same as those in (D).

the hRobo1 cytoplasmic protein (Figures 6A–6C). In contrast, a truncated form of the Flag-tagged hRobo1 cytoplasmic protein, lacking N-terminal residues 930–1173 was not significantly tyrosine phosphorylated in Cos1 cells also transfected with AblΔSH3 (Figures 6A and 6B). Thus, although this truncated protein is highly expressed, it does not act as a substrate for Abl, suggesting that the juxtamembrane region of hRobo1 contains the principal phosphotyrosine sites. The sequence that is deleted in the shorter protein contains tyrosine 1073 of the conserved CC1 motif (PTPYATT). This motif resembles the c-Abl phosphorylation site in c-Crk (PGPYAQP) (Feller et al., 1994; Rosen et al., 1995).

To map potential sites of tyrosine phosphorylation, nano-electrospray-tandem mass spectrometry was used to identify tryptic phosphopeptides from a GST-hRobo1 (residues 962–1217) fusion protein that had been phosphorylated in vitro using purified Abl. This analysis identified three phosphotyrosine sites in the membrane proximal region of the hRobo1 cytoplasmic domain, namely Y1073, located in the conserved CC1 motif (PTPYATT), the more N-terminal Y1038, located in the sequence STVYGDV of hRobo1 (GTDYAEV in dRobo1), and the more C-terminal Y1114, within the motif PVQYNIV of hRobo1 (HSPYSDA in dRobo1) (data not shown). Substitution of the tyrosine in CC1 (Y1073) with phenylalanine, or deletion of the CC1 motif (ΔCC1, removing residues 1070–1079) leads to a significant reduction in the tyrosine phosphorylation of the hRobo1 cytoplasmic domain by AblΔSH3 in the Cos1 cell cotransfection assay (Figures 6D and 6E). Additionally, there was a decrease in the gel mobility of the wild-type cytoplasmic hRobo1 protein upon phosphorylation by AblΔSH3, which was not evident for the Y1073F or ΔCC1 mutant proteins coexpressed with activated Abl, consistent with the possibility that Y1073 is phosphorylated by Abl in cells. These observations suggest that hRobo1 can be phosphorylated by the Abl tyrosine kinase at multiple sites within the juxtamembrane region, including Y1073 in the CC1 motif, both in vitro and in cultured cells. Together with the partial kinase dependence of the Abl gain-of-function phenotype and the kinase dependence of the Abl/Robo genetic interactions, these data support the idea that Abl could antagonize Robo function by directly phosphorylating it. Analysis of the effects of transgenic expression of a Y-F mutation of the tyrosine in CC1 further supports this suggestion (see below).

Transgenic Expression of Mutant Forms of Robo

To determine if the ΔCC mutations in the cytoplasmic domain that effect the binding of Robo to Abl and Ena effect the in vivo function of Robo, we expressed them transgenically in *Drosophila* using the *GAL4-UAS* system. We did the same for the Y-F point mutant that leads to decreased in vitro tyrosine phosphorylation by Abl (Figure 7A). We put the ΔCC deletion mutant transgenes into a *robo* mutant background and compared their ability to rescue *robo* function with that of wild-type *robo* transgenes. All three of the ΔCC mutant Robo constructs showed some ability to rescue *robo* loss of function, reducing the amount of ectopic midline crossing when expressed in a *robo* mutant background (Figure 7; Table 2; and data not shown), indicating that none of the three CC motifs are absolutely required for complete Robo repulsive output.

However, when compared with the rescue observed using wild-type transgenes, there were significant differences seen in the relative degree of rescue. Both the ΔCC2 and ΔCC3 mutants showed consistent reduction in their ability to rescue the *robo* phenotype. The differences were most striking in the case of the ΔCC2 mutant (Figures 7E and 7F; Table 2). In *robo* null mutants, the innermost Fas II positive pathway wanders back and forth across the midline (Figure 7D). When a wild-type Robo transgene is expressed in all CNS neurons in this background, the midline phenotype is restored to near wild type (Figure 7E). In contrast to the near complete rescue observed for the wild-type and ΔCC1 transgenes,

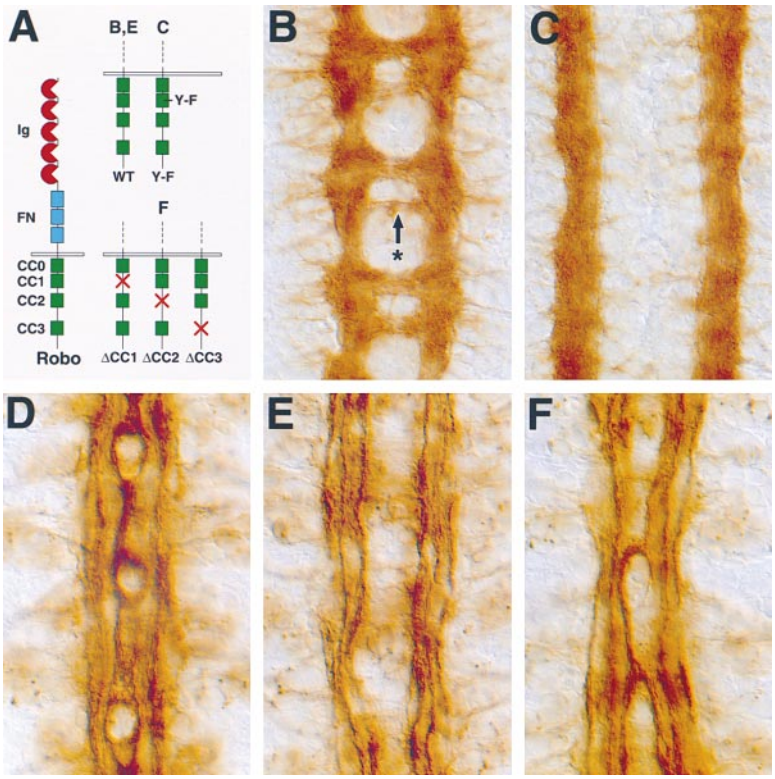

Figure 7. Transgenic Expression of Robo Cytoplasmic Domain Mutants

(A) A schematic diagram of the Robo receptor and the various cytoplasmic domain mutants generated for this study. The CC motifs are indicated by green boxes. The letters above each form of the cytoplasmic domain indicate the figure panel in which the form is shown.

(B and C) Stage 16 embryos stained with Mab BP102. Anterior is up. (B) A *2X UASrobo/elavGAL4* embryo. A mild phenotype is generated in which some commissures appear thinner than normal (arrow with asterisk). (C) A *UASroboY-F/elavGAL4* embryo. Commissures are completely absent.

(D) A stage 16 *robo* mutant stained with anti-Fas II Mab. The pCC pathway can be seen wandering back and forth across the midline.

(E) A stage 16 *robo* mutant rescued with *UASrobo*. The pCC pathway no longer crosses the midline.

(F) A stage 16 *robo* embryo rescued with *UASroboΔCC2*. Several Fas II bundles can still be observed ectopically crossing the midline.

robo mutants that express the ΔCC2 mutant transgene still exhibit moderate *robo* phenotypes in which many Fas II axon bundles still cross the midline (Figure 7F). Similar, but weaker effects are seen in the case of the ΔCC3 mutant (Table 2). The fact that the ΔCC1 mutant showed no reduction in its ability to rescue the *robo* mutant is consistent with the idea that CC1 is a site of negative regulation by Abl. The impaired ability of the ΔCC2 mutant to rescue *robo* function further supports a direct role for Ena in Robo repulsion.

In contrast to all wild-type *robo* transgenes examined thus far, several independent inserts of the *roboY-F* mutant transgene generate a completely commissureless phenotype when expressed in single copy (Figure 7C). Animals that express a relatively higher transgene dose of wild-type *UASrobo* (two copies of *UASrobo* and one copy of *elavGAL4*) have only a mild phenotype in which some commissures appear somewhat thinner (Figure 7B). Semi-quantitative immuno-histochemical comparison of the Robo protein levels of these two genotypes, indicate that *UASrobo2X* actually expresses relatively more protein than *UASroboY-F*, and that both forms of Robo exhibit a similar degree of axonal localization (data not shown). These observations suggest that RoboY-F functions as a dominant active form of Robo, that is able to repel all axons from the Slit-expressing midline (i.e., is still ligand-gated), at relatively lower protein levels than wild-type Robo.

Table 2. Comparative Rescue of *robo* Mutants with Wild-Type and ΔCC Mutant Transgenes

Genotype[1]	Animals scored	Phenotypic Classes[2]		
		Class I wild type	Class II mild *robo*	Class III moderate *robo*
robo^{5}; *UASrobo* *robo*^{5}; *elavGAL4*	24	18 (75%)	5 (21%)	1 (4%)
robo^{5}; *UASroboΔCC1* *robo*^{5}; *elavGAL4*	29	17 (59%)	10 (34%)	2 (7%)
robo^{5}; *UASroboΔCC2* *robo*^{5}; *elavGAL4*	30	4 (13%)	11 (37%)	15 (50%)
robo^{5}; *UASroboΔCC3* *robo*^{5}; *elavGAL4*	23	7 (30%)	12 (52%)	4 (18%)

[1] Multiple inserts of each of the different transgenes were examined for their ability to rescue *robo*. Different lines of each transgene behaved similarly and the data were pooled. Three independent lines each for *UASrobo, UASroboΔCC1,* and *UASroboΔCC2* were examined. Two lines of *UASroboΔCC3* were examined.

[2] The data were grouped into three phenotypic classes: Class I (wild type), animals that had 0-2 ectopic Fas II axon bundles crossing the midline; Class II (mild *robo*), animals that had 3-4 ectopic Fas II axon bundles crossing the midline; Class III (moderate *robo*), animals with 5 or more ectopic Fas II axon bundles crossing the midline.

In combination with the in vitro phosphorylation data and the genetic interactions of *abl* and *robo*, these results support a model in which Abl can directly antagonize Robo signaling by the phosphorylation of Robo at tyrosine 1040 (1073 in hRobo1). It will be of interest to determine whether additional sites of Robo tyrosine phosphorylation are also functionally significant. It should be stressed that although the in vitro, transgenic, and genetic interaction data are consistent with the proposed role of Abl in regulating Robo function, they do not directly prove that this interaction occurs in the organism. This will require future analysis of in vivo Robo tyrosine phosphorylation and determination of the effect of mutations in *abl* and/or overexpression of Abl on Robo phosphorylation.

Discussion

In this paper, we have identified Abl and Ena as complementary components of the signaling machinery downstream of the Robo repulsive axon guidance receptor. Genetic interactions indicate that loss of *ena* function partially disrupts Slit- and Robo-mediated repulsion from the midline. Limiting or removing *ena* function enhances partial loss-of-function *robo* phenotypes and suppresses *robo* gain-of-function phenotypes. In contrast, reduction of *abl* has the opposite consequence, suppressing the effects of a partial loss of *robo* function, while panneural overexpression of Abl antagonizes Robo function, leading to a phenotype resembling that of *robo* mutants.

Both Abl and Ena bind directly to Robo's cytoplasmic domain in vitro and Robo can act as a substrate for Abl kinase activity in vitro and in cell culture. Robo and Ena also show in vivo physical interactions. Furthermore, cytoplasmic domain mutants that reduce Ena binding to Robo result in impaired ability to rescue *robo* loss of function, while a Y-F mutation in a conserved tyrosine that can be phosphorylated by Abl in vitro has the opposite consequence, generating a hyperactive Robo receptor. These genetic and biochemical data support a model in which Abl and Ena play direct and opposing roles in the transmission of Robo's repulsive signal.

The implication of Ena in repulsive axon guidance is somewhat surprising in light of the previous results from the pathogen *Listeria monocytogenes* indicating that Mena is required for *Listeria's* actin-polymerization dependent motility. The *Listeria* data, together with Ena/VASP proteins in vitro effects on actin, has frequently been interpreted to suggest that Ena/VASP proteins function to promote actin polymerization, thereby promoting motility. On the contrary, our results indicate that Ena is partially required for axon repulsion from the midline. These data suggest that Ena may have the opposite function, namely, to inhibit forward growth cone motility at sites where Robo encounters Slit.

In a companion paper (Bear et al., 2000), an independent study in mammalian cell culture has reached a similar conclusion. By expressing a multimerized EVH1 domain binding site attached to specific subcellular localization sequences, Ena/VASP family members can be efficiently targeted to different areas of cultured fibroblasts. This system has allowed a direct examination of the role of Ena/VASP proteins in cell motility. Surprisingly, when Ena/VASP proteins are directed away from the cell membrane, using a mitochondrial targeting sequence, the cells actually migrate more quickly. Conversely, targeting Ena/VASP proteins to the membrane, or overexpressing Mena, leads to a dose-dependent decrease in the rate of cell migration. A major conclusion of this study is that Ena/VASP proteins function in part to decrease the rate of whole cell motility. Whether Ena/VASP proteins achieve the observed in vivo effects on whole cell and growth cone motility by stimulating or inhibiting actin polymerization awaits future investigation.

Ena Function Does Not Account for All of Robo Repulsion

While the dosage-sensitive genetic interactions between *ena* and *robo* support a role for Ena in midline repulsion, Ena clearly can not explain all of Robo's repulsive output. Indeed, although mild midline crossing defects are observed in *ena* mutants, on the whole, Robo-mediated repulsion works fairly well in the absence of Ena. In this light, it is perhaps not surprising that the Robo ΔCC2 mutant receptor (in which the Ena binding site is deleted) still provides some repulsive activity and can partially rescue *robo* loss-of-function mutants. These results indicate that there must be other proteins that function downstream of Robo to mediate repulsion. One would predict that simultaneously removing *ena* and the as yet unknown additional factors would reveal stronger disruptions of midline repulsion.

Thus, Ena is only part of what must be a more complex repulsive output from Robo. Ena helps strengthen the output (perhaps by locally putting the break on the actin-based motility machinery), but is only part of the output. In this light, it is interesting to note that Robo2 also binds Slit and mediates repulsion (albeit apparently more weakly than Robo), but Robo2 does not have the Ena binding site and does not bind Ena (J. Simpson, personal communication).

An important question for future studies concerns whether Ena is always docked on Robo, or alternatively, whether Slit binding to Robo leads to the recruitment of Ena to Robo's cytoplasmic domain. From what we know about other receptor systems, this second alternative seems more likely, but is an open question and needs to be directly tested.

Abl Phosphorylation and the Regulation of Robo Signaling

Our genetic analysis shows that Abl antagonizes Robo-mediated repulsion. The two most likely possibilities are that Abl functions to antagonize this pathway by phosphorylating Robo or by phosphorylating Ena. Three results argue in favor of a direct interaction with Robo. First, we observe certain kinds of dose-dependent genetic interactions between *abl* and *robo* that we do not observe between *abl* and *ena*, suggesting that the Abl and Robo proteins might directly interact. Second, our biochemical experiments have shown that Abl can directly phosphorylate Robo's cytoplasmic domain at one or more tyrosine residues. Third, a Y-F mutation in a conserved tyrosine that can be phosphorylated by Abl

in vitro generates a hyperactive Robo receptor. Taken together, these genetic and biochemical data suggest that it is the dephosphorylated form of Robo which is most active.

How might Abl normally regulate the output of Robo signaling? On the one hand, Abl-mediated phosphorylation might normally modulate the output of Robo signaling. Alternatively, this phosphorylation might participate more directly in the ligand-gated signal. It is interesting to speculate that it is the binding of Robo to its ligand Slit that triggers dephosphorylation, and that this in turn activates the repulsive response.

The CNS-specific receptor protein tyrosine phosphatases (RPTPs) RPTP10D and 69D are candidates to be additional factors that contribute to Robo repulsion. Simultaneous removal of these two RPTPs results in substantial ectopic midline crossing, and the double mutant shows dose-sensitive genetic interactions with *slit* (Sun et al., 2000). Whether these two phosphatases interact directly with Robo and whether their phosphatase activity is required for their observed roles in repulsion await future investigation.

In the model presented above, it is attractive to speculate that these two RPTPs function in opposition to the Abl kinase activity by directly dephosphorylating Robo upon Robo's interaction with Slit. Interestingly, the other two Robo family members in *Drosophila* (Robo2 and Robo3; J. Simpson, personal communication) share the phosphorylation sites in Robo that are phosphorylated by Abl in vitro. In addition, genetic interactions are observed between the RPTPs and Robo2 (J. Simpson, personal communiacation). Together these observations suggest that perhaps a common mechanism is employed to regulate the signaling output of the three Robo receptors. It will be of interest to determine the in vivo significance of the conserved tyrosine phosphorylation sites in the three Robo receptors. The future elucidation of the events set in motion by ligand binding will require the development of cell culture systems that will allow analysis of the phosphorylation state and cytoplasmic domain associations of the Robo receptors before and after Slit stimulation.

Robo Signaling Components Are Likely to Function in a Similar Fashion in Many Other Pathways

In addition to their function during Robo signaling shown here, it is clear that both Abl and Ena function in multiple guidance signaling pathways, and thus that they are not committed to repulsion downstream of Robo. In the nematode *C. elegans*, *ena* acts as a suppressor of the axon migration defects associated with ectopic expression of the UNC5 repulsive Netrin receptor (Colavita and Culotti, 1998). This raises the possibility that *ena* functions downstream of diverse repulsive guidance receptors.

In *Drosophila*, during motor axon pathfinding, *ena* and *abl* play roles in ISNb choice point control (Wills et al., 1999). Overexpression of *abl* or loss of *ena* generate an ISNb "bypass" phenotype, where the ISNb fails to defasciculate and branch off at the appropriate location to enter its muscle target region. This phenotype is also observed in mutations in *Dlar*, the gene encoding a receptor protein tyrosine phosphatase (RPTP) (Krueger et al., 1996). Mutations in all three of these genes (*ena, abl, and Dlar*) give rise to only partially penetrant ISNb guidance phenotypes and appear to modulate guidance decisions at this choice point.

At the midline, mutations in the genes encoding the ligand (Slit) and a key receptor (Robo) have strong and highly penetrant midline guidance phenotypes. In contrast, mutations in the genes encoding Ena, Abl, and RPTP10D and RPTP69D on their own have weaker and less penetrant phenotypes. This is consistent with Abl and the RPTPs modulating Robo receptor output, and Ena mediating only part of Robo output. If we apply this same logic to the motor axon ISNb choice point, then it is likely that some of the key components are still missing. At present, the only gene with a nearly 100% penetrant bypass phenotype at this choice point is *sidestep* (Sink and Goodman, 1994). Side is an Ig superfamily transmembrane protein that is expressed on muscle surfaces and appears to function as an attractive ligand for motor axons (H. Sink, personal communication). The Side receptor is not known. Whether the key receptor is the Side receptor or not, it is likely that the major growth cone receptor for the ISNb choice point has not yet been identified.

In this context, it is tempting to speculate, by analogy with the proposed model for Robo signaling, that at the ISNb motor axon choice point, DLAR and Abl play complementary roles in modulating the output activity of the hypothetical guidance receptor, while Ena functions as part of the receptor output. In this way, the two guidance decisions—to cross or not to cross the midline, and to fasciculate or defasciculate from other motor axons —use different signals on the outside of the growth cone, but similar signaling and regulatory mechanisms on the inside. We suggest that once the signal crosses the membrane, in both cases the output is regulated in opposing directions by Abl vs. one or more RPTPs, and that the output is partially mediated by Ena. This model provides a unifying way of viewing signal transduction during these two different guidance decisions. It will be interesting in the future to see to what degree this model holds up in terms of both the role of phosphorylation in modulating receptor output, and the role of Ena in mediating part of repulsive signaling.

Experimental Procedures

Genetics

The following stocks were created: 1) *ena^{GC1}/CyoWgβgal;elavGAL4,* 2)*robo^{1}/CyoWgβgal; elavGAL4*, 3)*slit^{2}/CyoWgβgal; elavGAL4*, 4)*EPabl, elavGAL4/TM3actinβgal,* 5) *ena^{GC1},EProbo2/CyOWgβgal*, 6)*ena^{210}/CyoWgβgal;UASrobo1B,3D,* 7)*ena^{GC1}/CyOWgβgal;UASrobo,elavGAL4/TM6βgal* 8) *ena^{GC1}/CyoWgβgal; UASfra-robo,elavGAL4/TM2,* 9) *ena^{GC1}/CyoWgβgal;2X UASfra-robo*. The following stocks were also used: *abl^{1},red,e/TM3actinβgal, abl^{4},red,e/TM3actinβgal, comm^{1}/TM3actinβgal*, *slit^{1}robo^{5}/CyoWgβgal*, *elavGAL4* and *scabrousGAL4*.

Transgenic lines of *UASrobo-myc, UASroboΔCC1-myc, UASroboΔCC1, UASroboΔCC2-myc, UASroboΔCC2, UASroboΔCC3-myc, UASroboΔCC3, UASroboY-F, UASroboΔC* were created. *UASrobo* and *UASroboΔCmyc* were made previously. *UASabl* and *UASabl^{kinasedead}* were obtained from David Van Vactor. The EP insert in *abl* (EP3101) came from a screen of the EP collection provided by the Rubin lab. A double mutant *robo^{4}, ena^{GC1}* chromosome was made by recombination. *robo^{1}*, *robo^{4}*, *robo^{5}*, *ena^{210}* and *ena^{GC1}*, *ena^{GC5}*, *ena^{GC8}* were kept over a *wingless(Wgβgal)* balancer chromosome.

Molecular Biology

The pharmacia pGEX system was used for GST fusions of the Abl SH2, Abl SH3, Ena, Ena EVH1, and Robo cytoplasmic domain constructs. Regions of interest were amplified by PCR, or subcloned using native restriction sites. CC mutants and the Y-F point mutant were made using Stratagene's ExSite mutagenesis kit. CC1 deletes residues 1037–1046. CC2 deletes residues 1104–1119. CC3 deletes residues 1262–1269. Novagen's pCite was used to make Robo plasmids for in vitro translation. All PCR constructs were sequenced. Human GST-fusion constructs were made by subcloning hRobo1 fragments (GST-hRobo1 1430–1651 and GST-hRobo1 962–1217) into pGEX-4T2. For expression in mammalian cells, the full-length hRobo1 cDNA was subcloned into pCDNA3.1 (Invitrogen). Flag-tagged mammalian expression constructs (hRobo1 cytoplasmic 930–1651, 1174–1651, and 1430–1651) were made by subcloning into pFLAG-CMV-2 (Kodak). hRobo1 cDNA mutants were made by PCR mutagenesis. All constructs were sequenced. GST fusion proteins were expressed and purified according to manufacturer's instructions. In vitro translation with S^{35}-labeled methionine was performed using Promega's TNT coupled transcription/translation rabbit reticulocyte lysate system.

Protein–Protein Interactions

Glutathione-Sepharose beads loaded with fusion proteins were equilibrated in binding buffer (20 mM HEPES-KOH [pH 7.9], 50 mM KCl, 2.5 mM $MgCl_2$, 10% Glycerol, 1 mM DTT, 0.2% NP40, and 1mM PMSF 1.5% goat serum) for 1 hr at 4°C. Equivalent GST loading was assessed by Coomassie staining of SDS-PAGE gels. For binding assays using in vitro translated proteins, 1/3 of a 50 μl reaction was added to equilibrated beads. Binding was overnight at 4°C on Nutator. Beads were washed several times in 10 mM Tris-HCl (pH 7.5), 150 mM NaCl, 1 mM EDTA, and 0.2% NP40 and separated on 12% SDS-PAGE gels. Gels were fixed for 30 min in 50% methanol, 10% glacial acetic acid, and 40% water and dried on a BioRad gel dryer and exposed to film for 2–24 hr, or for 2 hr on a BioRad phospho-imager screen. Input was normalized prior to binding, by quantitateing an aliquot of each translation reaction by Phosho-imager analysis. For S2 cell binding assays, 10 ml of Robo-expressing S2 cells were pelleted and lysed in 1 ml of cold lysis buffer for 2–3 min (20 mM HEPES-KOH [pH 7.9], 50 mM KCl, 2.5 mM $MgCl_2$, 10% Glycerol, 1 mM DTT, 1mM PMSF, 1 mM $NaVO_4$, and 0.5% Triton X-100), spun at 14000 rpm and transferred to a fresh tube. Ten to twenty milliliters of extract were used in each assay.

For Co-IP, extracts were prepared from 25–50 μl of wild-type embryos or embryos overexpressing one copy of *UASrobo-myc* or *UASroboΔCC2-myc*. Lysis and immunoprecipitation were performed in PBS/1% NP40 (or 0.8% Tween for Robo IPs), 1mM PMSF, and 1 μg/ml each of aprotinin and leupeptin. The monoclonal antibodies were coupled to protein A Sepharose beads with bridging antibody for 1 hr at room temperature. Binding was performed for 60–90 min at 4°C. Samples were washed three times in lysis buffer, separated on 8% PAGE gels, transferred to membranes, and blotted with anti-Robo or anti-Myc antibodies at 1:50 or anti-Ena antibodies at 1:200. Signal was detected using the ECL detection system and autoradiography.

Rabbit antibodies were raised against GST-hRobo1 (amino acids 1430–1651) and affinity purified from crude sera with the original antigen. Cells were lysed in 50 mM HEPES (pH 7.5), 150 mM NaCl, 10% glycerol, 1% Triton X-100, 1.5 mM $MgCl_2$, 1 mM EGTA, 100 mM NaF, 10 μg/ml aprotinin, 10 μg/ml leupeptin, 0.2 mM sodium orthovanadate, and 1 mM PMSF. Full-length hRobo1 or the cytoplasmic hRobo1 proteins were immunoprecipitated from the Triton X-100 soluble fraction with 1 μg/ml anti-hRobo1 polyclonal antibody and protein A Sepharose beads or 1 μg/ml anti-Flag M2 monoclonal antibody (Sigma) and goat anti-mouse agarose beads, respectively, for 1.5 hr at 4°C. Immunoprecipitates were washed three times (20 mM HEPES [pH 7.5], 150 mM NaCl, 10% glycerol, 0.1% Triton X-100, 5 μg/ml aprotinin, 5 μg/ml leupeptin, 0.2 mM sodium orthovanadate, and 1 mM PMSF), separated by SDS-PAGE, and blotted with anti-phosphotyrosine monoclonal antibody (Upstate Biotechnology) at 0.5 μg/ml. Western blots were stripped in 0.1 M glycine (pH 2.5) and reprobed with anti-Flag M2 monoclonal antibody at 1.5 μg/ml.

Mammalian Cell Culture

Cos1 cells were cultured in Dulbecco's modified Eagle medium containing 10% FBS. Cells were transfected using lipofectin reagent (Gibco BRL) overnight, after which time the media was replaced. Cells were harvested 48 hr after replacement of the media.

Phosphopeptide Mapping

GST-hRobo1 962–1217 was phosphorylated in vitro with purified v-Abl (Oncogene Research Products). Kinase reactions were performed using 3–25 units of v-Abl/μg of GST-hRobo1 fusion protein at 37°C for 30 min (in 20 mM $MgCl_2$, 0.2 mM DTT, 60 mM HEPES [pH 7.5], 2 mM ATP, and 20 μg/ml BSA). Protein was trypsin digested at 37°C for 4 hr using a 50:1 ratio of protein to protease. Peptides were desalted using ZipTip columns (Millipore), equilibrated in 5% formic acid, washed with equilibration buffer and eluted in 60% methanol/5% formic acid. MS/MS analysis was performed on the QSTAR mass spectrometer (PE-Sciex) with a nanoelectrospray source (Protana A/S). Product ion spectra were generated by collisionally induced dissociation (CID). Sequencing was performed using PeptideScan (EMBL). The following three fragments were found to be tyrosine phosphorylated: (1) QTNLMLPESTVYGDVDLSNK, (2) FVNPSGQPTPYATTQLIQSNLSNNMNNGSGDSGEK, and (3) QEVA PVQYNIVEQNK.

Immunohistochemistry and Antibody Production

Embryo staining and monoclonal antibody production procedures (Ena amino acids 105–370) were as previously described (Kidd et al., 1998a).

Acknowledgments

We thank Beth Blankmeier, Ron Smith, and Wei-Yu Chen for outstanding technical assistance. We thank David Van Vactor and Zak Wills for providing *abl* and *ena* stocks, and also for Abl and Ena antibodies. Shawn Ahern-Djamali and Michael Hoffman kindly provided *ena* stocks and the pCiteEna plasmid. We thank Kim Bland for Robo-expressing S2 cells. Julie Simpson provided critical comments on the manuscript. We thank Kai Zinn for valuable discussions. We are grateful to Kathleen Binns for assistance with mass spectrometry. D. M. was supported by a fellowship from NSERC. Work supported by a grant from the Medical Research Council of Canada and an HHMI International Scholar Award to T. P. Supported by NIH grant NS18366 and grant #GBC-1-9801 from the Christopher Reeve Paralysis Foundation (both to C. S. G.). G. J. B. is a Postdoctoral Fellow supported by the Cancer Research Fund of the Damon Runyon-Walter Winchell Foundation (#DRG 1474). C. S. G. is an Investigator with the Howard Hughes Medical Institute.

Received January 31, 2000; revised May 16, 2000

References

Bachmann, C., Fischer, L., Walter, U., and Reinhard, M. (1999). The EVH2 domain of the vasodilator-stimulated phosphoprotein mediates tetramerization, F-actin binding, and actin bundle formation. J. Biol. Chem. *274*, 23549–23557.

Bashaw, G.J., and Goodman, C.S. (1999). Chimeric axon guidance receptors: the cytoplasmic domains of slit and netrin receptors specify attraction versus repulsion. Cell *97*, 917–926.

Bear, J.E., Libova, I., Loureiro, J.J., Jürgen, W., and Gertler, F.B. (2000). Negative regulation of fibroblast motility by Ena/VASP proteins. Cell *101*, this issue, 717–728.

Brose, K., Bland, K.S., Wang, K.H., Arnott, D., Henzel, W., Goodman, C.S., Tessier-Lavigne, M., and Kidd, T. (1999). Slit proteins bind Robo receptors and have an evolutionarily conserved role in repulsive axon guidance. Cell *96*, 795–806.

Colavita, A., and Culotti, J.G. (1998). Suppressors of ectopic UNC-5 growth cone steering identify eight genes involved in axon guidance in Caenorhabditis elegans. Dev. Biol. *194*, 72–85.

Elkins, T., Zinn, K., McAllister, L., Hoffmann, F.M., and Goodman, C.S. (1990). Genetic analysis of a *Drosophila* neural cell adhesion

molecule: interaction of fasciclin I and Abelson tyrosine kinase mutations. Cell *60*, 565–575.

Feller, S.M., Knudsen, B., and Hanafusa, H. (1994). c-Abl kinase regulates the protein binding activity of c-Crk. EMBO J. *13*, 2341–2351.

Gertler, F.B., Bennett, R.L., Clark, M.J., and Hoffmann, F.M. (1989). *Drosophila* abl tyrosine kinase in embryonic CNS axons: a role in axonogenesis is revealed through dosage-sensitive interactions with disabled. Cell *58*, 103–113.

Gertler, F.B., Comer, A.R., Juang, J.L., Ahern, S.M., Clark, M.J., Liebl, E.C., and Hoffmann, F.M. (1995). enabled, a dosage-sensitive suppressor of mutations in the Drosophila Abl tyrosine kinase, encodes an Abl substrate with SH3 domain-binding properties. Genes Dev. *9*, 521–533.

Gertler, F.B., Niebuhr, K., Reinhard, M., Wehland, J., and Soriano, P. (1996). Mena, a relative of VASP and Drosophila Enabled, is implicated in the control of microfilament dynamics. Cell *87*, 227–239.

Henkemeyer, M., West, S.R., Gertler, F.B., and Hoffmann, F.M. (1990). A novel tyrosine kinase-independent function of *Drosophila* abl correlates with proper subcellular localization. Cell *63*, 949–960.

Hong, K., Hinck, L., Nishiyama, M., Poo, M.M., Tessier-Lavigne, M., and Stein, E. (1999). A ligand-gated association between cytoplasmic domains of UNC5 and DCC family receptors converts netrin-induced growth cone attraction to repulsion. Cell *97*, 927–941.

Jackson, P., and Baltimore, D. (1989). N-terminal mutations activate the leukemogenic potential of the myristolated form of c-*abl*. EMBO J. *8*, 449–456.

Kidd, T., Bland, K.S., and Goodman, C.S. (1999). Slit is the midline repellent for the robo receptor in *Drosophila*. Cell *96*, 785–794.

Kidd, T., Brose, K., Mitchell, K.J., Fetter, R.D., Tessier-Lavigne, M., Goodman, C.S., and Tear, G. (1998a). Roundabout controls axon crossing of the CNS midline and defines a novel subfamily of evolutionarily conserved guidance receptors. Cell *92*, 205–215.

Kidd, T., Russell, C., Goodman, C.S., and Tear, G. (1998b). Dosage sensitive and complementary functions of Roundabout and Commissureless control axon crossing of the CNS midline. Neuron *20*, 25–33.

Krueger, N.X., Van Vactor, D., Wan, H.I., Gelbart, W.M., Goodman, C.S., and Saito, H. (1996). The transmembrane tyrosine phosphatase DLAR controls motor axon guidance in *Drosophila*. Cell *84*, 611–622.

Lanier, L.M., Gates, M.A., Witke, W., Menzies, A.S., Wehman, A.M., Macklis, J.D., Kwiatkowski, D., Soriano, P., and Gertler, F.B. (1999). Mena is required for neurulation and commissure formation. Neuron *22*, 313–325.

Laurent, V., Loisel, T.P., Harbeck, B., Wehman, A., Gröbe, L., Jockusch, B.M., Wehland, J., Gertler, F.B., and Carlier, M.F. (1999). Role of proteins of the Ena/VASP family in actin-based motility of Listeria monocytogenes. J. Cell Biol. *144*, 1245–1258.

Li, H.S., Chen, J.H., Wu, W., Fagaly, T., Zhou, L., Yuan, W., Dupuis, S., Jiang, Z.H., Nash, W., Gick, C., et al. (1999). Vertebrate slit, a secreted ligand for the transmembrane protein roundabout, is a repellent for olfactory bulb axons. Cell *96*, 807–818.

Loisel, T.P., Boujemaa, R., Pantaloni, D., and Carlier, M.F. (1999). Reconstitution of actin-based motility of Listeria and Shigella using pure proteins. Nature *401*, 613–616.

Reinhard, M., Giehl, K., Abel, K., Haffner, C., Jarchau, T., Hoppe, V., Jockusch, B.M., and Walter, U. (1995). The proline-rich focal adhesion and microfilament protein VASP is a ligand for profilins. EMBO J. *14*, 1583–1589.

Rørth, P. (1996). A modular misexpression screen in Drosophila detecting tissue-specific phenotypes. Proc. Natl. Acad. Sci. USA *93*, 12418–12422.

Rosen, M.K., Yamazaki, T., Gish, G.D., Kay, C.M., Pawson, T., and Kay, L.E. (1995). Direct demonstration of an intramolecular SH2-phosphotyrosine interaction in the Crk protein. Nature *374*, 477–479.

Seeger, M., Tear, G., Ferres-Marco, D., and Goodman, C.S. (1993). Mutations affecting growth cone guidance in *Drosophila*: genes necessary for guidance toward or away from the midline. Neuron *10*, 409–426.

Sink, H., and Goodman, C.S. (1994). Mutations in *sidestep* lead to defects in pathfinding and synaptic specificity during the development of neuromuscular connectivity in Drosophila. Soc. Neurosci. Abst. *20*, 1283.

Sun, Q., Bahri, S., Schmid, A., Chia, W., and Zinn, K. (2000). Receptor tyrosine phosphatases regulate axon guidance across the midline of the *Drosophila* embryo. Development *127*, 801–812.

Tessier-Lavigne, M., and Goodman, C.S. (1996). The molecular biology of axon guidance. Science *274*, 1123–1133.

Wills, Z., Marr, L., Zinn, K., Goodman, C.S., and Van Vactor, D. (1999a). Profilin and the Abl tyrosine kinase are required for motor axon outgrowth in the *Drosophila* embryo. Neuron *22*, 291–299.

Wills, Z., Bateman, J., Korey, C.A., Comer, A., and Van Vactor, D. (1999b). The tyrosine kinase Abl and its substrate enabled collaborate with the receptor phosphatase Dlar to control motor axon guidance. Neuron *22*, 301–312.

Zallen, J.A., Yi, B.A., and Bargmann, C.I. (1998). The conserved immunoglobulin superfamily member SAX-3/Robo directs multiple aspects of axon guidance in *C. elegans*. Cell *92*, 217–227.